Highly selective room temperature ammonia gas sensors based on d-band C-SnO_2 and response behavior induced by oxidative and reductive role shifts

Hongmin Zhu [a], *Hanyang Ji* [a], *Zhenyu Yuan* [a, b, c, d] *, *Yanbai Shen* [e], *Hongliang Gao* [a, b, c, d], *Fanli Meng* [a, b, c, d] *

a. College of Information Science and Engineering, Northeastern University, Shenyang 110819, China

b. Hebei Key Laboratory of Micro-Nano Precision Optical Sensing and Measurement Technology, Qinhuangdao, 066004, China

c. National Frontiers Science Center for Industrial Intelligence and Systems Optimization, Northeastern University, Shenyang 110819, China

d. Key Laboratory of Data Analytics and Optimization for Smart Industry (Northeastern University), Ministry of Education, China

e. School of Resources and Civil Engineering, Northeastern University, Shenyang 110819, China

*Corresponding authors: Fanli Meng (mengfanli@ise.neu.edu.cn), Zhenyu Yuan (yuanzhenyu@ise.neu.edu.cn).

1. Experiment

1.2. Computation method and model

The electronic structure of the material and the interaction of the material with the gas are analyzed through density functional theory. The Dmol3 code was also used to calculate the adsorption energy of the target gas on the material with the Basis set as DND. The electron exchange correlations were established via GGA (generalized gradient approximation) and PEB (Perdew Burke enzehr) models [1, 2]. The (110) face is the most stable face of SnO_2 and an important site for catalysis and gas sensitization [3, 4]. Therefore, the cleave surface of the SnO_2 calculation model was chosen to be the (110) face, as shown in Fig. S3. 3 x 2 supercell models were adopted with vacuum thickness of 15 Å, K-point grid of 1 x 1 x 1, smearing of 0.005 Ha and global orbital cutoff of 4.0 Å. The model energy was set to 1 x 10^5 Ha, the force converge was set to 0.002 Ha/Å and the displacement was set to 0.005 Å. In every model, bottom layer is fixed and rest all layers and adsorbate are fully relaxed.

The adsorption energy of the target gas on the material was calculated through equation (2) [5].

$$E_{ads} = E_{materials + gas} - E_{materials} - E_{gas} \quad (2)$$

Where $E_{materials+gas}$, $E_{materials}$ and E_{gas} were system energy of material adsorption gas, material system energy and gas molecular energy, respectively.

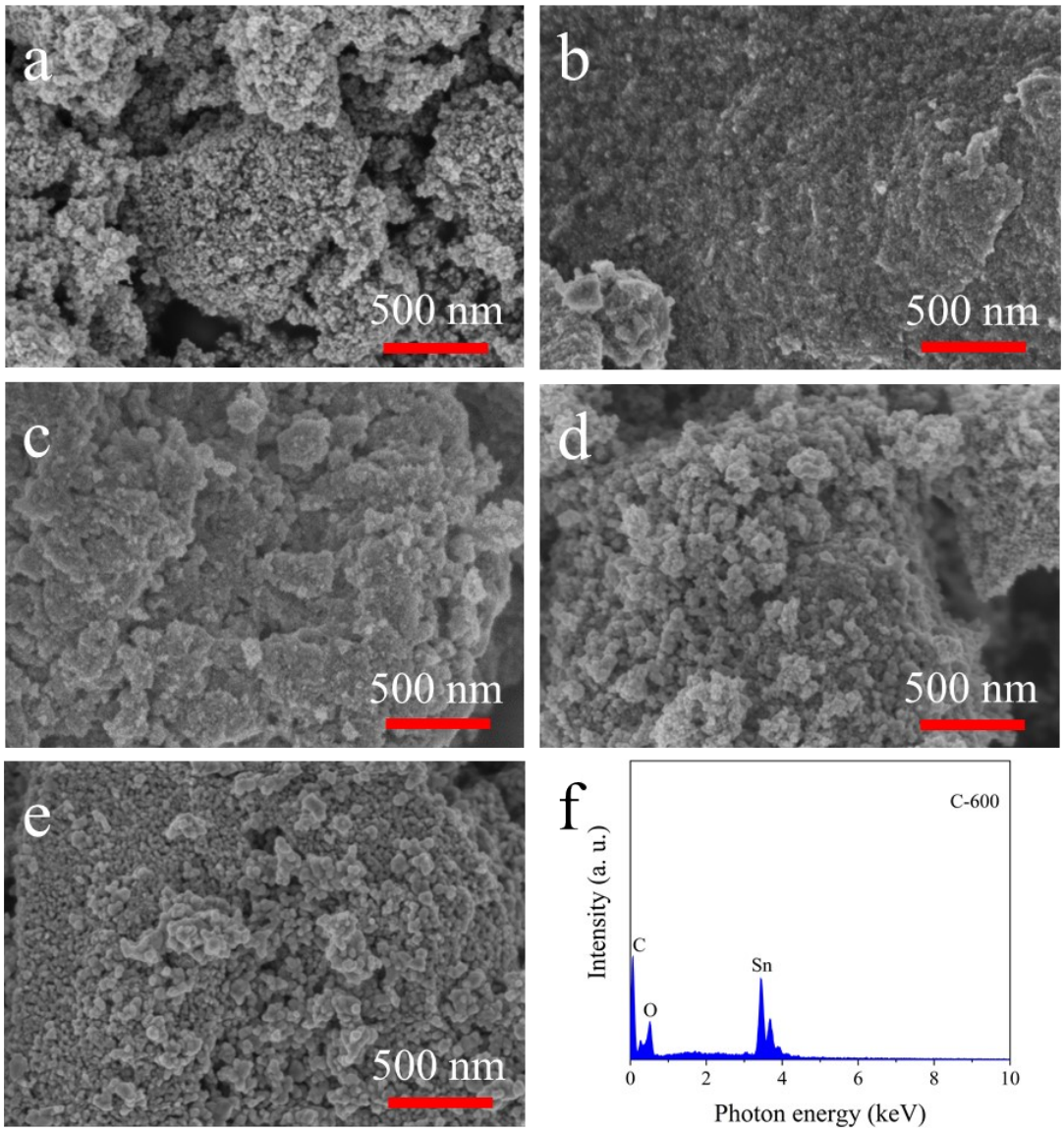

Fig. S1. SEM of (a) W-600, (b) C-300, (c) C-500, (d) C-600, and (e) C-800, and (f) DES of C-600.

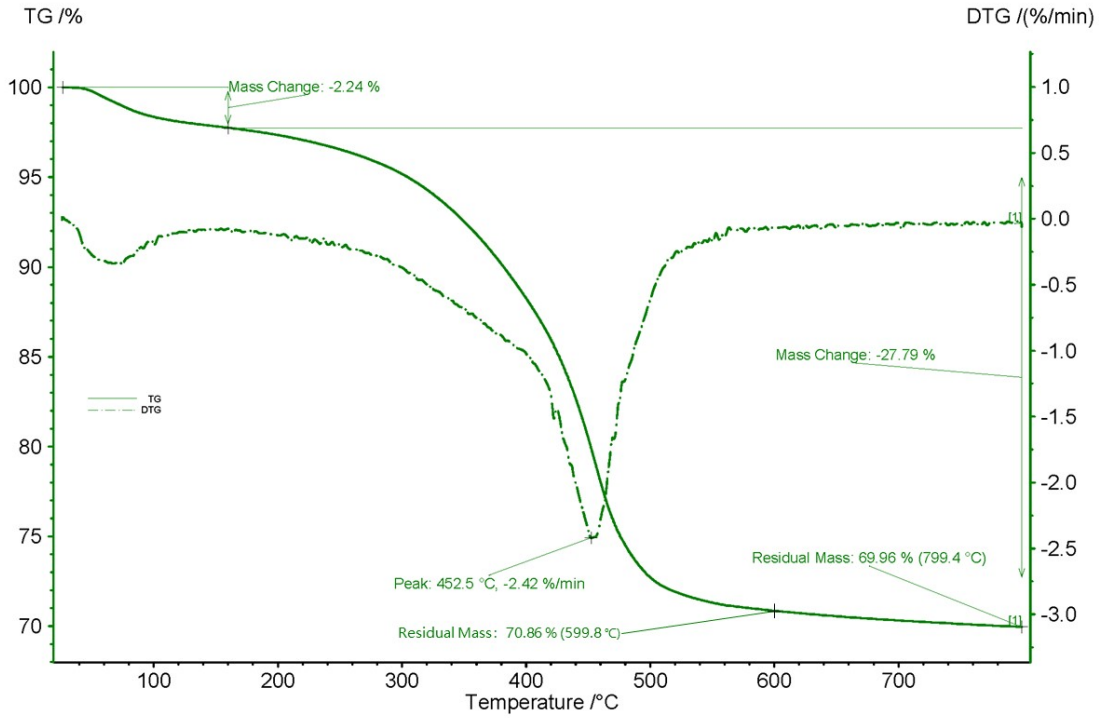

Fig.S2. TG and DTG curves of C and Sn complex precursor materials.

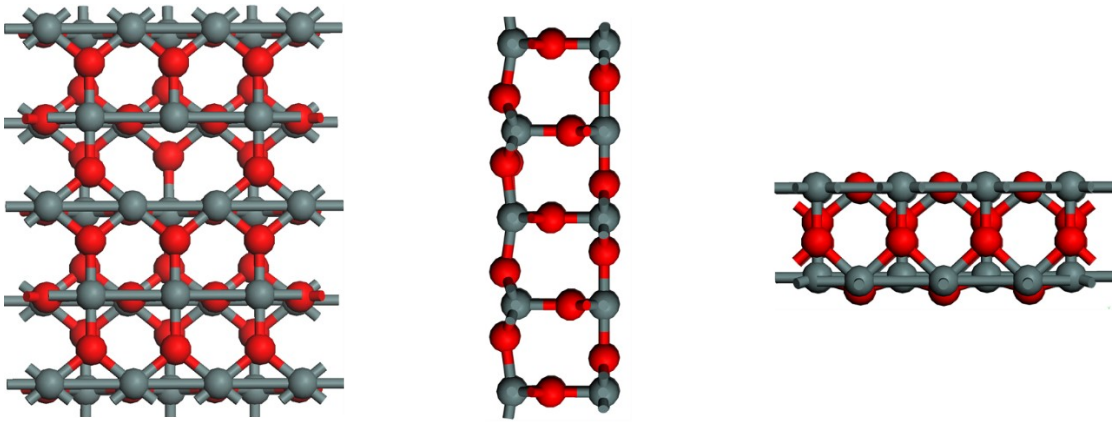

Fig.S3. Three views of the SnO_2 (110) surface crystal model.

Tab.S1. The gap between the HOMO of the material and the LUMO of NH_3, and the HOMO of the materials. And the gap between the LUMO of the material and the HOMO of NH_3, and the LUMO of the materials.

Configuration	HOMO	LUMO of NH_3-HOMO	LUMO	LUMO-HOMO of NH_3
NH_3	-5.624		0.349	
SnO_2	-3.425	3.774	-3.220	2.404
C1-SnO_2	-3.422	3.771	-3.113	2.511
C2-SnO_2	-3.423	3.772	-3.112	2.512
C3-SnO_2	-3.421	3.770	-3.112	2.512
C4-SnO_2	-3.439	3.788	-3.081	2.543
C5-SnO_2	-3.668	4.017	-3.521	2.103

Tab.S2. The gap between the HOMO of the material with -COOH and the LUMO of NH_3, and the HOMO of the materials with -OCOO-. And the gap between the LUMO of the material with -COOH and the HOMO of NH_3, and the LUMO of the materials with -OCOO-.

Configuration	HOMO	LUMO of NH_3-HOMO	LUMO	LUMO-HOMO of NH_3
SnO_2-OCOO-	-3.933	4.282	-3.427	2.197
C1-SnO_2-OCOO-	-3.909	4.258	-3.437	2.187
C2-SnO_2-OCOO-	-3.909	4.258	-3.437	2.187
C3-SnO_2-OCOO-	-3.920	4.269	-3.375	2.249
C4-SnO_2-OCOO-	-3.920	4.269	-3.375	2.249
C5-SnO_2-OCOO-	-3.850	4.199	-3.628	1.996

Tab.S3. The gap between the HOMO of the material with -COOH and the LUMO of NH_3, and the HOMO of the materials with -COOH. And the gap between the LUMO of the material with -COOH and the HOMO of NH_3, and the LUMO of the materials with -COOH.

Configuration	HOMO	LUMO of NH_3-HOMO	LUMO	LUMO-HOMO of NH_3
SnO_2-OCOO-	-3.503	3.852	-3.286	2.338
C1-SnO_2-OCOO-	-3.505	3.854	-3.171	2.453
C2-SnO_2-OCOO-	-3.501	3.850	-3.247	2.377
C3-SnO_2-OCOO-	-3.502	3.851	-3.248	2.376
C4-SnO_2-OCOO-	-3.505	3.854	-3.171	2.453
C5-SnO_2-OCOO-	-3.737	4.086	-3.481	2.143

References

[1] W. Yu, J. Zhang, T. Peng, New insight into the enhanced photocatalytic activity of N-, C- and S-doped ZnO photocatalysts, Applied Catalysis B: Environmental, 181(2016) 220-7.

[2] H. Tang, L.N. Sacco, S. Vollebregt, H. Ye, X. Fan, G. Zhang, Recent advances in 2D/nanostructured metal sulfide-based gas sensors: mechanisms, applications, and perspectives, Journal of Materials Chemistry A, 8(2020) 24943-76.

[3] G. Li, S. Li, Z.-K. Han, C. Zou, H. Wu, W. Yuan, et al., In Situ Resolving the Atomic Reconstruction of SnO_2 (110) Surface, Nano Letters, 21(2021) 7309-16.

[4] L. Zhang, M. Cong, X. Ding, Y. Jin, F. Xu, Y. Wang, et al., A Janus Fe-SnO_2 Catalyst that Enables Bifunctional Electrochemical Nitrogen Fixation, Angew Chem Int Ed Engl, 59(2020) 10888-93.

[5] J. Zhao, B. Liu, L. Meng, S. He, R. Yuan, Y. Hou, et al., Plasmonic control of solar-driven CO_2 conversion at the metal/ZnO interfaces, Applied Catalysis B: Environmental, 256(2019) 117823.